Published in final edited form as:
Automatica (Oxf). 2009 March ; 45(3): 736–743. doi:10.1016/j.automatica.2008.09.023.

Identification of a Modified Wiener-Hammerstein System and Its Application in Electrically Stimulated Paralyzed Skeletal Muscle Modeling

Er-Wei Bai[a], **Zhijun Cai**[a], **Shauna Dudley-Javorosk**[b], and **Richard K. Shields**[b]

[a] Dept. of Electrical and Computer Engineering, University of Iowa, Iowa City, Iowa 52242

[b] Graduate Program in Physical Therapy and Rehabilitation Science, University of Iowa, Iowa City, Iowa 52242

Abstract

Electrical muscle stimulation demonstrates potential for restoring functional movement and preventing muscle atrophy after spinal cord injury (SCI). Control systems used to optimize delivery of electrical stimulation protocols depend upon mathematical models of paralyzed muscle force outputs. While accurate, the Hill-Huxley-type model is very complex, making it difficult to implement for real-time control. As an alternative, we propose a modified Wiener-Hammerstein system to model the paralyzed skeletal muscle dynamics under electrical stimulus conditions. Experimental data from the soleus muscles of individuals with SCI was used to quantify the model performance. It is shown that the proposed Wiener-Hammerstein system is at least comparable to the Hill-Huxley-type model. On the other hand, the proposed system involves a much smaller number of unknown coefficients. This has substantial advantages in identification algorithm analysis and implementation including computational complexity, convergence and also in real time model implementation for control purposes.

Keywords

system identification; nonlinear systems; wiener-hammerstein systems; medical applications

1 Introduction

After spinal cord injury (SCI), the loss of volitional muscle activity triggers a range of deleterious adaptations. Muscle cross-sectional area declines by as much as 45% in the first 6 weeks after injury, with further additional atrophy occurring for at least 6 months [1]. Muscle atrophy impairs weight distribution over bony prominences, predisposing individuals with SCI to pressure ulcers which is potentially a life-threatening secondary complication [2]. The diminution of muscular loading through the skeleton precipitates severe osteoporosis in paralyzed limbs. The lifetime fracture risk for individuals with SCI is

Email addresses: er-wei-bai@uiowa.edu (Er-Wei Bai), zhijun-cai@uiowa.edu (Zhijun Cai), shauna-dudley@uiowa.edu (Shauna Dudley-Javorosk), richard-shields@uiowa.edu (Richard K. Shields).

*This paper was not presented at any IFAC meeting. The work was supported in part by NSF ECS-0555394 and NIH/NIBIB EB004287. The corresponding author E.W. Bai, Tel:+3193355949 and Fax: +3193356028

twice the risk experienced by the non-SCI population [3]. Rehabilitation interventions to prevent post-SCI muscle atrophy and its sequel are an urgent need.

Electrical muscle stimulation after SCI is an effective method to induce muscle hypertrophy [4], [7], fiber type and metabolic enzyme adaptations [5], [6], and improvements in torque output and fatigue resistance [7],[8], [9]. New evidence suggests that an appropriate longitudinal dose of muscular load can be an effective anti-osteoporosis countermeasure [7], [10]. Electrical muscle stimulation also has potential utility for restoration of function in tasks such as standing, reaching, and ambulating. The myriad applications for electrical stimulation after SCI have created a demand for control systems that adjust stimulus parameters in real-time to accommodate muscle output changes (potentiation, fatigue) or inter-individual force production differences. To facilitate the refinement of control system algorithms, mathematical models or system identification of muscle torque output are continuously being developed to successfully adapt stimulus parameters to real-time muscle output changes.

Over the last decades, researchers have developed a number of muscle models aimed at modeling muscle force outputs [11], [12], [13]. The Hill-Huxley-type model [12] is the most advanced and accurate model so far [14], [15]. Compared to other models, the Hill-Huxley-type model represents muscle dynamics well. However, its complexity undermines its usefulness for real time implementation for control. Identification of a Hill-Huxley-type model is non-trivial because it is time-varying, high dimensional and nonlinear. Local minimum versus global minimum is always a difficult issue for Hill-Huxley model identification. Users must tune identification algorithm parameters patiently (including the initial estimates) in order to have a good result.

Our goal is to develop a model that is comparable to or outperforms the Hill-Huxley-type model, but at a much reduced complexity. We propose a modified Wiener-Hammerstein system that resembles the Hill-Huxley-type structure but has a much smaller number of unknown parameters and enjoys a high degree of accuracy. The purpose of this work is to describe the modified Wiener-Hammerstein system for modeling paralyzed skeletal muscle dynamics under electrical stimulation. By using actual soleus force data from 14 subjects with SCI, we demonstrate that advantages of the proposed model over previous models are theoretically justified and experimentally verified. Equally important is another demonstration of the usefulness of block oriented nonlinear systems in a real world application.

2 Problem statement and collection of SCI patient data

Fourteen subjects with chronic SCI provided written informed consent, as approved by the University of Iowa Human Subjects Institutional Review Board. A detailed description of the stimulation and force transducing system has been previously reported [7], [8], [9], (Figure 1). In brief, a subject sat in a wheelchair with the knee and ankle positioned at ninety degrees. The foot rested upon a rigid metal plate, and the ankle was secured with a soft cuff and turnbuckle connectors. Padded straps over the knee and forefoot ensured isometric conditions. The tibial nerve was supramaximally stimulated in the popliteal fossa using a nerve probe and a custom computer-controlled constant-current stimulator. Stimulation was controlled by digital pulses from a data-acquisition board (Metrabyte DAS 16F, Keithley Instruments Inc., Cleveland, OH) housed in a microcomputer under custom software control. The simulator was programmed to deliver a 10-pulse train (15 Hz train with duration 667ms). The electrical stimulation input and the corresponding muscle force output are recorded as shown in Figure 2. 15 Hz stimulus is justified for two reasons. First, recall that we design the muscle stimulus training protocol according to three main design criteria: to

"overload" the muscle to induce hypertrophy, to repetitively stress the muscle to increase endurance, and to exceed a dose of compressive load hypothesized to be osteogenic for the distal tibia. In a previous study [23] of the torque frequency relationship of acutely and chronically paralyzed muscle, it was reported that these goals can be achieved by 15 Hz stimulus because muscular overload (60% of maximal torque) can be generated via 15 Hz supra-maximal stimulus. Secondly, the purpose of the modeling is for the subsequent subjects controlled exercise with work-rest cycles. It was reported that eliciting muscle contractions with an 1 on 2 off work-rest cycle (Burke like protocol) with 15 Hz frequency induces significant low-frequency fatigue without compromising neuromuscular transmission [7].

The purpose of identification or modeling is to find a model which predicts the output based on the input in some optimal ways.

3 Hill-Huxley-type model

Among several muscle models developed in the last two decades [11], [12], [13], the Hill-Huxley-type model [12] is the most advanced and accurate one [14], [15]. The Hill-Huxley-type nonlinear model describes the stimulated muscle behavior in the continuous time domain by means of two time varying nonlinear differential equations (3.1) and (3.2) connected nonlinearly

$$\frac{dC_N}{dt}=\frac{1}{\tau_c}\sum_{i=1}^{n}R_i\exp(-\frac{t-t_i}{\tau_c})-\frac{C_N}{\tau_c}, \quad (3.1)$$

where $R_i=1+(R_0-1)\exp(-\frac{t-t_i}{\tau_c})$

$$\frac{dy}{dt}=A\frac{C_N}{K_m+C_N}-\frac{y}{\tau_1+\tau_2\frac{C_N}{K_m+C_N}}. \quad (3.2)$$

In (3.1) and (3.2), t_i is the time of ith stimulus input and C_N is the (internal) variable, while $y(t)$ is the force output. Note that no actual input amplitude is directly used but only the input time sequence t_i is used. The effect of the input amplitude is automatically adjusted by the parameters R_i and τ_c. The model incorporates six parameters A, R_0, and K_m as gains, and τ_1, τ_2 and τ_c as the time constants as well as a sequence of coefficients t_i's that describe the exact time and the interval of electrical pulse inputs.

Note there is a pure delay d between the electrical stimulus and the force response. Rigorously speaking, the model is a function of delay. Practically, however, this delay is usually first detected and then compensated in identification. Therefore, the delay does not explicitly appear in the model.

4 Modified Wiener-Hammerstein system

For easy implementation of digital computers and equipments, our model is in the discrete time domain. The input $u(kT)$ is the electrical stimulus (in volts) at time kT where $T = 0.2$ ms is the sampling interval and the output $y(kT)$ is the muscle force at time kT.

The proposed modified Wiener-Hammerstein system is shown in Figure 3(a) with the nonlinearity $w = f(v)$ denoted by $\frac{Av}{1+Bv}$, where B and A are unknown parameters which vary

for each individual subject. The internal signals $v(kT)$ and $w(kT)$ are unavailable for identification purpose.

The model in Figure 3 is expressed in terms of z-transform which can be written equivalently as

$$v((k+1)T)=a_1 v(kT)+a_2 u(kT) \quad (4.1)$$

$$y((k+1)T)=b_1 y(kT)+b_2 w(kT). \quad (4.2)$$

While the parameters B and A in the nonlinear block are necessary to account for individual variations, the overall system in Figure 3(a) is however unnecessary. Observe that the nonlinear block in the middle of Figure 3(a) can be decomposed into three blocks, two constant gains and a known nonlinearity, as shown in Figure 3(b). Further, the gains B and A/B can be absorbed by the linear systems, which results in the system in Figure 3(c), where $a_2 = a_0 B$ and $b_2 = b_0 \frac{A}{B}$. This normalization process greatly simplifies the identification problem, reducing the number of unknown parameters from six to four. It is important to comment that the system in Figure 3(c) is identical to the system in Figure 3(a) from input to output point of view, though the complexity is greatly reduced.

So far, the model is a standard Wiener-Hammerstein system [17], [18], [20], [19], [21], [22] with four unknown parameters. From the actual input and output response shown in Figure 2, it is obvious that the output drops exponentially when the input stimulus is no longer present. The decrease of the output in this region can be well modeled by a first order linear system with zero input. This observation can be incorporated into the choice of a_1. To this end, we set

$$a_1=\begin{cases} a_1, & t \le \tau \\ 0, & t>\tau \end{cases} \quad \text{and } \tau=t_{last}+1/15+2d \quad (4.3)$$

where t_{last} is the end time of the last input pulse, $1/15(sec)$ is the time interval between two pulses and d is the delay between the input and output which was detected before identification as done in the Hill-Huxley-type model case. The idea behind this choice of a_1 is that a new input pulse should have arrived at $\tau = t_{last} + 1/15 + 2d$ if the input stimulus continues. If the input stimulus stops, the model should be switched to reflect exponential drop $y((k+1)T) = b_1 y(kT)$ as shown in Figure 2. This is no longer a standard Wiener-Hammerstein mode but has a linear time varying block in which the pole a_1 switches from a non-zero value to zero after input stops. We call this model a modified Wiener-Hammerstein system.

We comment that applications of the block oriented nonlinear systems including Hammerstein and Wiener models for skeletal muscle modeling are not new and have been proposed [13,14,16]. In [16], a Hammerstein model was suggested which was simple but the performance was not satisfactory. In [13] and later in [14], a time-varying Wiener-Hammerstein model was proposed. It contains two systems inter-connected by a nonlinear static block. To accommodate individual variations, the nonlinear static block has two unknown parameters. Unlike the model proposed in this paper, however, there two parameters can not be absorbed by dynamic systems resulting in a larger number of unknown parameters. Further, to compensate exponential drops of the output in the absence of the input, a nonlinear time varying equation with three unknown parameters was used in [13] while the proposed model in this paper uses a switched linear system with two

parameters. In summary, the model of [13] has a similar complexity as the Hill-Huxley model including the same number of unknown parameters and thus, suffers from the same complexity related issues in identification. The model proposed in this paper, that can be viewed as an improvement over the model of [13], has a much reduced complexity and at the same time, outperforms the Hill-Huxley model which is well documented [15] to perform better than or at least to be comparable with the model of [13].

5 Identification algorithm and convergence analysis

Let $\theta = [a_1, a_2, b_1, b_2]$ denote the unknown system parameters of the modified Wiener-Hammerstein system and &*thetas;* = $[\hat{a}_1, \hat{a}_2, \hat{b}_1, \hat{b}_2]$ its estimate. Let $\hat{y}(kT)$ be the predicted output calculated using the estimates

$$\widehat{y}(kT)=\frac{\widehat{b}_2}{z-\widehat{b}_1} f\left(\frac{\widehat{a}_2}{z-\widehat{a}_1} u(kT)\right), \quad (5.4)$$

where z is the z-transform, i.e., $z^{-1}y(kT) = y((k-1)T)$, and $f(x)=\frac{x}{1+x}$ is the known nonlinearity. Further, from the stability and physiology constraints, we may set $0 < a_1, a_2, b_1 \leq 1$ and $0 < b_2$. Now the identification problem is to find the best parameter set $\theta^*=[a_1^*, a_2^*, b_1^*, b_2^*]$ which minimizes the sum of squared errors between the actual output $y(kT)$ and the predicted output $\hat{y}(kT)$ of the proposed model

$$\begin{aligned}\theta^* &= \arg\min_{\widehat{\theta}} J(\widehat{a}_1, \widehat{a}_2, \widehat{b}_1, \widehat{b}_2) \\ &= \arg\min_{\widehat{\theta}} \left\{\sum_k (y(kT) - \widehat{y}(kT))^2\right\}\end{aligned} \quad (5.5)$$

subject to $0 < \hat{a}_1, \hat{b}_1 \leq 1$ and $0 < \hat{a}_2, \hat{b}_2$, where $y(kT)$ is the actual force output.

Obviously, because (5.5) is nonlinear, local minimum versus global minimum is always an issue. We solve this problem by utilizing the structure of the proposed model and then design an identification algorithm which guarantees the global minimum. The idea is to divide this 4-dimensional problem into an 1-dimensional and a 2-dimension problems in two stages.

Let s be the minimum integer that satisfies $sT \geq \tau$. Suppose the values of $\hat{a}_1$ and $\hat{a}_2$ are given, the internal signal

$$\widehat{w}(kT)=\begin{cases} f\left(\frac{\widehat{a}_2}{z-\widehat{a}_1} u(kT)\right) & k \leq s \\ 0 & k>s \end{cases}$$

can be calculated, where $\hat{w}$ depends on the choice of $\hat{a}_1$ and $\hat{a}_2$. Based on this internal signal and the model $\hat{y}((k+1)T) = \hat{b}_1\hat{y}(kT) + \hat{b}_2\ \hat{w}(kT)$ or equivalently

$$\widehat{y}(kT)=\begin{cases} \sum_{i=0}^{k-1} \widehat{b}_1^{k-1-i}\widehat{b}_2\widehat{w}(iT) & k \leq s \\ \widehat{b}_1^{k-s}\sum_{i=0}^{s-1} \widehat{b}_1^{s-1-i}\widehat{b}_2\widehat{w}(iT) & k>s \end{cases}$$

the optimal $\hat{b}_1$ and $\hat{b}_2$ with given values of $\hat{a}_1$ and $\hat{a}_2$ are the solution of

$$[\widehat{b}_1^*, \widehat{b}_2^*] = \arg \min_{[\widehat{b}_1, \widehat{b}_2]} \{ \sum_{k=1}^{s} [(y(kT) - \sum_{i=0}^{k-1} \widehat{b}_1^{k-1-i} \widehat{b}_2 \widehat{w}(iT)]^2 + \sum_{k=1}^{N-s} [(y((k+s)T - \widehat{b}_1^k \sum_{i=0}^{s-1} \widehat{b}_1^{s-1-i} \widehat{b}_2 \widehat{w}(iT)]^2 \} \quad (5.6)$$

By taking derivative of the cost function with respect to $\hat{b}_2$ and setting it to zero yields

$$\widehat{b}_2 = g(\widehat{b}_1) = \frac{\sum_{k=1}^{s} [y(kT) \sum_{i=0}^{k-1} \widehat{b}_1^{k-1-i} \widehat{w}(iT)] + \sum_{k=1}^{N-s} [y((k+s)T) \widehat{b}_1^k \sum_{i=0}^{s-1} \widehat{b}_1^{s-1-i} \widehat{w}(iT)]}{\sum_{k=1}^{s} (\sum_{i=0}^{k-1} \widehat{b}_1^{k-1-i} \widehat{w}(iT))^2 + \sum_{k=1}^{N-s} (\widehat{b}_1^k \sum_{i=0}^{s-1} \widehat{b}_1^{s-1-i} \widehat{w}(iT))^2} \quad (5.7)$$

Now replacing $\hat{b}_2$ by $g(\hat{b}_1)$, (5.6) becomes 1-dimensional,

$$\min J_2(\widehat{b}_1) = \min \sum_{k=1}^{N} (y(kT) - \widehat{y}(kT, \widehat{b}_1))^2 \quad (5.8)$$

for fixed $\hat{a}_1$ and $\hat{a}_2$. Since (5.8) is 1-dimensional, the global minimum can be easily detected by plotting the cost function versus $\hat{b}_1 \in (0, 1]$ as shown in Figure 4 for Subject 1 data. Then, the optimal $\hat{b}_2$ is obtained from $\hat{b}_1$ as in (5.7). This process guarantees a unique optimal pair $[\widehat{b}_1^*, \widehat{b}_2^*] = h(\widehat{a}_1, \widehat{a}_2)$ for given $\hat{a}_i$, $i = 1, 2$, and the minimization problem (5.5) of four parameters becomes the minimization problem of two parameters

$$\min J(\widehat{a}_1, \widehat{a}_2, h(\widehat{a}_1, \widehat{a}_2)). \quad (5.9)$$

Similarly, the optimization (5.9) is 2-dimensional and the cost function J versus $\hat{a}_1$ and $\hat{a}_2$ can be easily plotted and visualized as shown in Figure 5 illustrated by Subject 1 data where clearly the global minimum lies in the region $a_1 \in [0.95, 1]$ and $a_2 \in (0, 0.1]$. Then any nonlinear optimization algorithm can be use to find the global minimum locally as shown in Figure 6. This demonstrates that though the original optimization is 4-dimensional and nonlinear, the algorithm developed guarantees the global minimum. We now summarize the algorithm as follows.

Identification algorithm: Given the data set $u(kT)$, $y(kT)$, $k = 1, 2, ..., N$.

Step 1: For each $\hat{a}_1$ and $\hat{a}_2$, find the optimal $\hat{b}_1$ of (5.8) or equivalently (5.6) substituting $\hat{b}_2 = g(\hat{b}_1)$. Calculate $\hat{b}_2$ from (5.7).

Step 2: Plot the cost function $J(\hat{a}_1\ \hat{a}_2, h(\hat{a}_1, \hat{a}_2))$ versus $0 < \hat{a}_1, \hat{a}_2 \leq 1$. Locate the region in which the global minimum lies.

Step 3: Apply any nonlinear optimization algorithm in this region to find the optimal $\hat{a}_1$ and $\hat{a}_2$, and compute the corresponding $\hat{b}_1$ and $\hat{b}_2$.

Theorem 5.1 *Consider the modified Wiener-Hammerstein model under the electrical stimulus. Then, the above identification algorithm produces* $0 < a_1^*, a_2^*, b_1^* \leq 1, 0 < b_2^*$ *that achieve the global minimum of* (5.5) *provided that*

$$\sum_{k=1}^{s} y(kT) \sum_{i=0}^{k-1} \widehat{b}_1^{k-1-i} \widehat{w}(iT) + \sum_{k=1}^{N-s} y((k+s)T) \widehat{b}_1^{k} \sum_{i=0}^{s-1} \widehat{b}_1^{s-1-i} \widehat{w}(iT) > 0 \quad (5.10)$$

Proof: For $0 < \hat{a}_1 \le 1$, $\hat{a}_2 \le 1$, $\hat{w}(kT)$ is always positive. The assumption (5.10) implies that the solution $\hat{b}_2$ of (5.7) is unique and positive. The rest of the proof follows from the discussion provided above.

We make two comments here.

- The assumption (5.10) is always satisfied in applications because $\hat{b}_1 > 0$, $\hat{w}(kT) > 0$ for $k \le s$ or $\hat{w}(kT) = 0$ for $k > s$ and the actual force output $y(kT)$ is dominantly positive and only in a negligible region $y(kT)$ could be negative with a very small magnitude as shown in Figure 2.
- The algorithm is designed to avoid local minimums at a price of efficiency. In the case that the optimization (5.6) has only one (local and global) minimum which is the case for all 14 subjects tested, solving the optimization (5.9) directly appears more efficient. Of course, success in all 14 subjects does not mean the optimization (5.6) always has only one minimum for all future subjects. For a practical application, we suggest to solve (5.9) directly first. Only if the fitting result is unsatisfactory that is an indication of local minimum, the above algorithm should be applied to avoid trapping in a local minimum. In our work, we use the modified MATLAB program ”fminsearchbnd” to solve the nonlinear optimization problem. The MAT-LAB program ”fminsearchbnd” is Nelder-Mead simplex approach based and is able to deal with simple upper-bound and lower-bound constraints.

6 Results and discussion

6.1 Comparison criteria

Comparisons are made against the Hill-Huxley-type nonlinear model, the most accurate model available in the literature. We identified both the modified Wiener-Hammerstein system and the Hill-Huxley-type model using soleus force data from subjects with SCI. The modified Wiener-Hammerstein system is identified based on the algorithm presented above. For identification of the Hill-Huxley-type nonlinear model, much care had to be taken to avoid a local minimum. To this end, the estimates were first manually tuned until the model output has a relatively good fit to the actual force output. Then the resultant parameters were used as initial values for ”fminsearch”, which refines the fitness further. The output of ”fminsearch” was further perturbed to generate a cluster of initial estimates which were fed into ”fminsearch” again. The best solution was considered as the Hill-Huxley-type model.

For comparison, the standard goodness-of-fit (gof)

$$\text{gof} = 1 - \sqrt{\frac{\sum_{k=1}^{N} (y(kT) - \widehat{y}(kT))^2}{\sum_{k=1}^{N} (y(kT) - \bar{y}(kT))^2}}, \quad (5.11)$$

and the normalized mean absolute error

$$\text{nmae}=\frac{\frac{1}{N}\sum_{k=1}^{N}|y(kT)-\widehat{y}(kT))|}{max\{y(kT)\}}. \quad (5.12)$$

are used, where N is the total number of data length, and $\hat{y}(kT)$ and $\bar{y}(kT)$ are the predicted force output by the model and the mean of the actual force output, respectively.

6.2 Fitting performance

Figure 7 and Figure 8 show the actual force outputs (solid), the predicted force outputs by the modified Wiener-Hammerstein (dashed) system and the Hill-Huxley-type model (dash-dotted), respectively, under 15 Hz electrical stimulus for fourteen subjects. The goodness-of-fits (gof) and the normalized mean absolute errors (nmae) are shown in Table 1. Table 2 shows identified parameters of the modified Wiener-Hammerstein model and the Hill-Huxley-type model. Though both the modified Wiener-Hammerstein model and the Hill-Huxley-type model provide excellent results, the proposed modified Wiener-Hammerstein system seems to perform slightly better for most subjects as shown in Figure 9 of the standard boxplot, where the boxes have lines at the lower quartile, median and upper quartile values. The whiskers are lines extending from each end of the box. Recall that the higher the better for gof and the lower the better for nmae.

6.3 Discussion

The utility of control systems for electrical stimulus of paralyzed muscle depends in a large measure on the fit capabilities of the underlying muscle model. Although the Hill Huxley model is the most advanced and accurate model in the literature, it is not easy to identify and is difficult to incorporate into real time control algorithms due to the number of parameters involved [15]. A simpler model with comparable fit capabilities would have greater usefulness in real patient exercise control applications. Compared to the Hill-Huxley-type model, the proposed Wiener-Hammerstein system possesses the following attractive properties.

- Simplicity: The proposed system consists of four parameters. On the other hand, the Hill-Huxley-type model is described by six unknown parameters.
- Competitive performance: Both the modified Wiener-Hammerstein system and the Hill-Huxley-type model provide good fitting performance. For all the fourteen subjects, the proposed modified Wiener-Hammerstein model performs slightly about 3% better in terms of goodness-of-fit (0.9398 vs. 0.9105) and 34% better in terms of normalized mean absolute error (0.0184 vs. 0.0278). In general, it is safe to say that the proposed modified Wiener-Hammerstein system is at least comparable to the Hill-Huxley-type model in terms of performance but with a smaller number of unknowns.
- Easy to Identify: The proposed modified Wiener-Hammerstein system together with its identification algorithm developed has no problem of local minimum while identification performance of the Hill-Huxley-type model relies heavily on the initial estimates. Therefore, some time-consuming and very fine adjustments have to be made in order to avoid the local minimum problem.

  A key in achieving the global minimum is a decomposition step that decomposes the original and higher dimensional optimization problem into an one dimensional problem $J(\hat{b}_1)$, $0 < \hat{b}_1 \leq 1$ and a two dimensional problem $J(\hat{a}_1, \hat{a}_2)$, $0 < a\hat{}_1, a\hat{}_2 \leq 1$. The decomposition is possible because of the structure of the proposed model. Then, these one and two dimensional problems are solved by an exhaustive search. Note that there is a huge difference between an exhaustive search of an one or two

dimensional problem and an exhaustive search of a higher dimensional problem simply because an one or two dimensional problem can be easily visualized. For instance, for solving min $J(\hat{b}_1)$, $0 < \hat{b}_1 \leq 1$, the objective function $J(\hat{b}_1)$, $0 < \hat{b}_1 \leq 1$, is plotted and the global minimum can be easily determined by a visual inspection. A similar statement can be made about min $J(\hat{a}_1, \hat{a}_2)$, $0 < \hat{a}_1, \hat{a}_2 \leq 1$. This observation is however not true for a general optimization problem of higher dimensions as the original problem or the one in the case of the Hill-Huxley model. Further, for both the one dimensional $J(\hat{b}_1)$ and two dimensional $J(\hat{a}_1, \hat{a}_2)$ problems, there is one and only one local (or global) minimum for all 14 subjects tested. Though not a proof, it seems to suggest that practically these one and two dimensional problems can be solved by any optimization algorithms and no exhaustive search is needed.

- Easy to implement: The ultimate goal of the skeletal muscle model is to be implemented in the control algorithm. The proposed modified Wiener-Hammerstein system possesses a smaller number of unknown parameters and requires much less computational expense. This makes the proposed system much easier to incorporate into a control scheme.

7 Conclusions

The proposed modified Wiener-Hammerstein model performs well compared to the most advanced and accurate Hill-Huxley-type model with a much smaller number of unknowns. It is a very competitive alternative in modeling skeletal muscle dynamics and has great potential to be incorporated into control systems, which we are working on currently. The identification algorithms developed accordingly are very efficient for paralyzed skeletal muscle modeling.

References

1. Castro MJ, Apple DF Jr, Hillegass EA, Dudley GA. Influence of complete spinal cord injury on skeletal muscle cross-sectional area within the first 6 months of injury. European Journal of Applied Physiology & Occupational Physiology. 1999; 80:373–378. [PubMed: 10483809]
2. Shields RK, Dudley-Javoroski S. Musculoskeletal deterioration and hemicorporectomy after spinal cord injury. Physical Therapy. 2003; 83:263–75. [PubMed: 12620090]
3. Vestergaard P, Krogh K, Rejnmark L, Mosekilde L. Fracture rates and risk factors for fractures in patients with spinal cord injury. Spinal Cord. 1998; 36:790–6. [PubMed: 9848488]
4. Mahoney ET, Bickel CS, Elder C, Black C, Slade JM, Apple D Jr, Dudley GA. Changes in skeletal muscle size and glucose tolerance with electrically stimulated resistance training in subjects with chronic spinal cord injury. Arch Phys Med Rehabil. 2005; 86:1502–1504. [PubMed: 16003691]
5. Crameri RM, Weston A, Climstein M, Davis GM, Sutton JR. Effects of electrical stimulation-induced leg training on skeletal muscle adaptability in spinal cord injury. Scandinavian Journal of Medicine & Science in Sports. 2002; 12:316–22. [PubMed: 12383078]
6. Andersen JL, Mohr T, Biering-Sorensen F, Galbo H, Kjaer M. Myosin heavy chain isoform transformation in single fibres from m. vastus lateralis in spinal cord injured individuals: effects of long-term functional electrical stimulation (FES). Pflugers Archiv - European Journal of Physiology. 1996; 431:513–8. [PubMed: 8596693]
7. Shields RK, Dudley-Javoroski S. Musculoskeletal plasticity after acute spinal cord injury: effects of long-term neuromuscular electrical stimulation training. J Neurophysiol. 2006; 95(4):2380–90. [PubMed: 16407424]
8. Shields RK, Dudley-Javoroski S. Musculoskeletal adaptation in chronic spinal cord injury: effects of long-term soleus electrical stimulation training. Journal of Neurorehabilitation and Neural Repair. 2006; 21:169–179.

9. Shields RK, Dudley-Javoroski S, Littmann AE. Post-fatigue potentiation of paralyzed soleus muscle: Evidence for adaptation with long-term electrical stimulation training. Journal of Applied Physiology. 2006; 101:556–565. [PubMed: 16575026]
10. Frey, Law LA.; Shields, RK. Mathematical models use varying parameter strategies to represent paralyzed muscle force properties: a sensitivity analysis. J Neuroengineering Rehabil. 2005; 2:12.
11. Ding J, Wexler AS, Binder-Macleod SA. A mathematical model that predicts the force-frequency relationship of human skeletal muscle. Muscle Nerve. 2002; 26:477–85. [PubMed: 12362412]
12. Ding J, Wexler AS, Binder-Macleod SA. Mathematical models for fatigue minimization during functional electrical stimulation. J Electromyogr Kinesiol. 2003; 13:575–88. [PubMed: 14573372]
13. Bobet J, Stein RB. A simple model of force generation by skeletal muscle during dynamic isometric contractions. IEEE Trans Biomed Eng. 1998; 45:1010–6. [PubMed: 9691575]
14. Bobet J, Gossen ER, Stein RB. A comparison of models of force production during stimulated isometric ankle dorsiflexion in humans. IEEE Trans Neural Syst Rehabil Eng. 2005; 13:444–51. [PubMed: 16425825]
15. Frey, Law LA.; Shields, RK. Mathematical models of human paralyzed muscle after long-term training. J Biomech. 2007:2597–2595.
16. Hunt KJ, Munih M, Donaldson NN, Barr FM. Investigation of the Hammerstein hypothesis in the modeling of electrically stimulated muscle. IEEE Trans Biomed Eng. 1998; 45:998–1009. [PubMed: 9691574]
17. Westwick D, Verhaegen M. Identifying MIMO Wiener systems using subspace model identification methods. Signal Processing. 1996; 52:235–258.
18. Voros J. Parameter identification of discontinuous Hammerstein systems. Automatica. 1997; 33:1141–1146.
19. Crama P, Schoukens J. Initial estimates of Wiener and Hammerstein systems using multisine excitation. IEEE Transactions on Instrumentation and Measurement. 2001; 50:1971–1975.
20. Bai EW, Li D. Convergence of the iterative Hammerstein system identification algorithm. IEEE Transactions on Automatic Control. 2004; 49:1929–1940.
21. Zhang, Q.; Iouditski, A.; Ljung, L. Identification of Wiener system with monotonous nonlinearity. presented at IFAC Symposium on System Identification; Newcastle: Australia. 2006.
22. Cerone V, Reguto D. Bounding the parameters of linear systems with input backlash. IEEE Transactions on Automatic Control. 2007; 52:531–536.
23. Shields R, CY-J. The effects of fatigue on the torque-frequency curve of the human paralyzed soleus muscle. Journal of Electromyogr Kinesiol. 1997; 7(1):3–13.

Biographies

Er-Wei Bai was educated in Fudan University, Shanghai Jiaotong University, both in Shanghai China, and the University of California at Berkeley. Dr. Bai is Professor of Electrical and Computer Engineering at the University of Iowa where he teaches and conducts research in identification, control, signal processing and their applications in engineering and medicine.

Dr. Bai is an IEEE Fellow and a recipient of the President's Award for Teaching Excellence.

Zhijun Cai was educated in Shanghai JiaoTong University, China, and Louisiana State University, USA. Dr. Cai is currently a research fellow in the Department of Electrical and Computer Engineering at the University of Iowa. His research interests include system modeling, adaptive/nonlinear control, signal processing and image processing.

Richard K. Shields PhD, PT was educated at the Mayo Clinic, Rochester Minnesota and the University of Iowa, Iowa City, Iowa. Dr. Shields is Professor of Physical Therapy and Rehabilitation Science in the Carver College of Medicine at the University of Iowa where he conducts research in neuromotor control after spinal cord injury.

Dr. Shields is an APTA Fellow and a recent recipient of the Williams Research Award. He also received the Collegiate Teaching and Mentoring Award from the Graduate College in 2000 and 2004, respectively.

Shauna Dudley-Javoroski received a Masters degree in Physical Therapy from the University of Iowa, where she is currently a PhD candidate in the Rehabilitation Science program. Her research interests include musculoskeletal plasticity after spinal cord injury, both during the initial atrophic phase and after administration of therapeutic loading interventions. She has a particular interest in musculoskeletal imaging techniques.

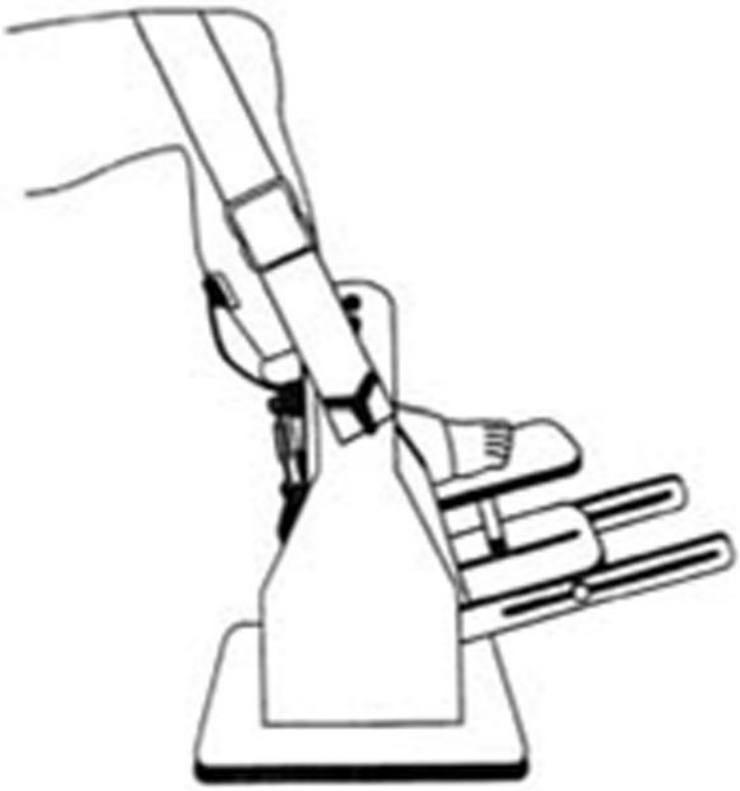

Fig. 1.
Schematic representation of the limb fixation and force measurement system.

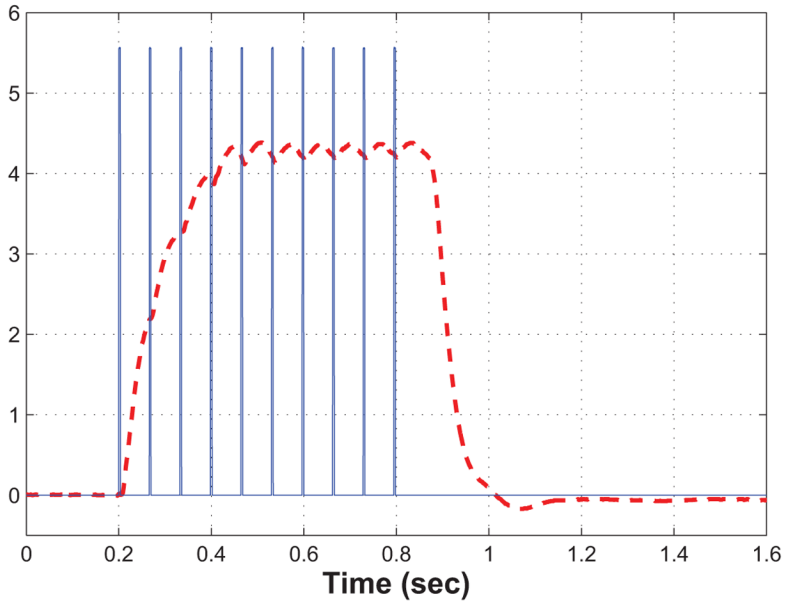

Fig. 2.
Electrical stimulus input(blue solid) and corresponding output (red dashed) at 15 Hz frequency.

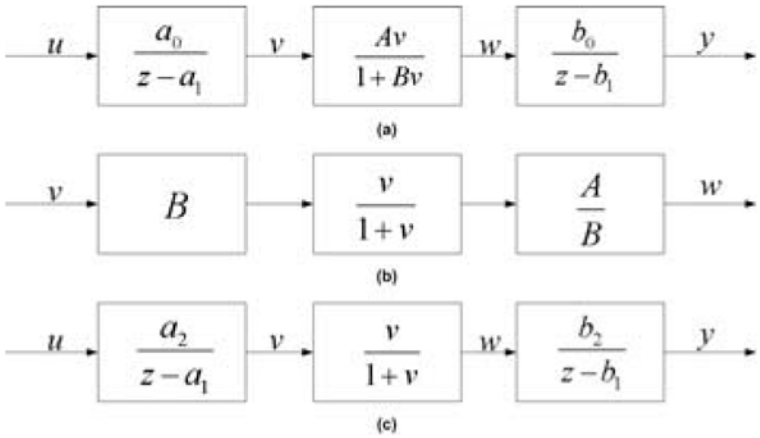

Fig. 3.
(a): Wiener-Hammerstein muscle model. (b): The middle nonlinear block of (a) can be decomposed into three parts. (c): The simplified Wiener-Hammerstein muscle model.

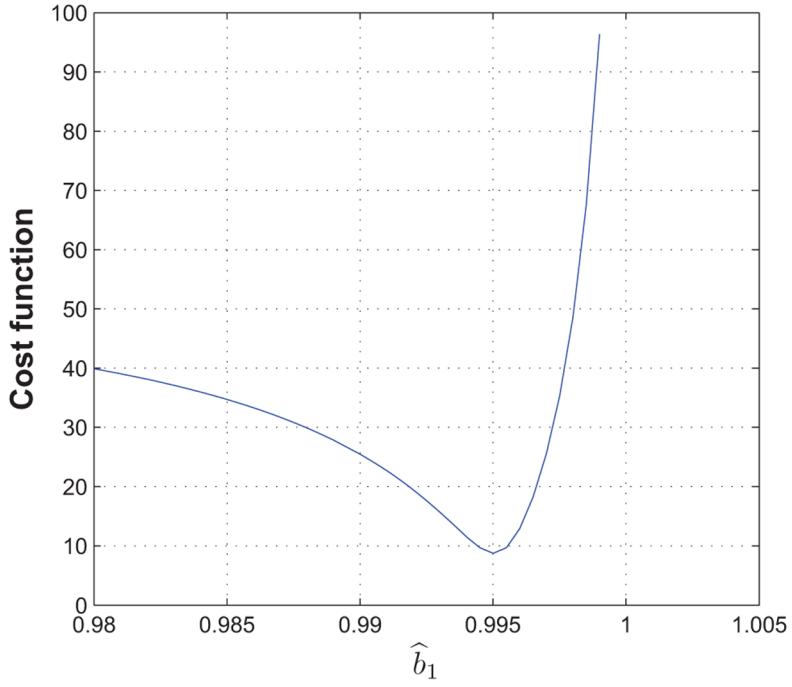

Fig. 4.
The cost function $J_2(\hat{b}_1)$ vs $\hat{b}_1$.

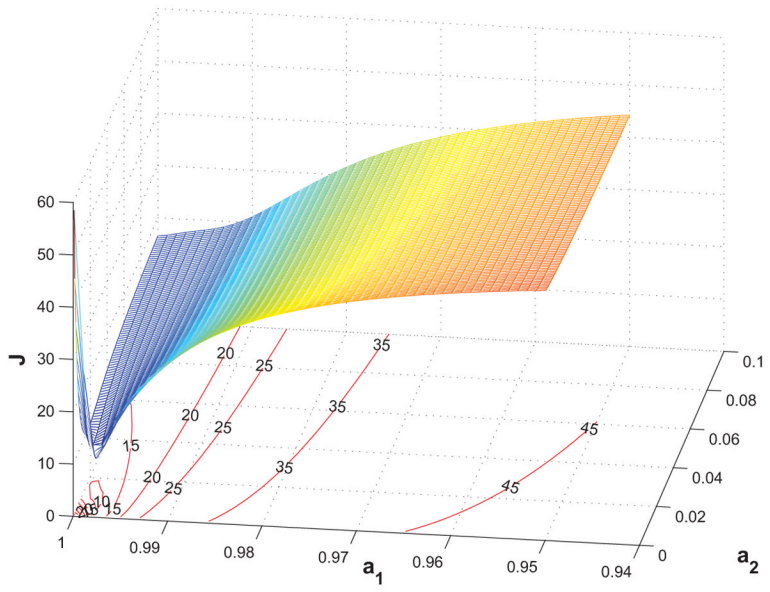

Fig. 5.
The cost function $J(a_1, a_2, h(a_1, a_2))$ vs a_1 and a_2.

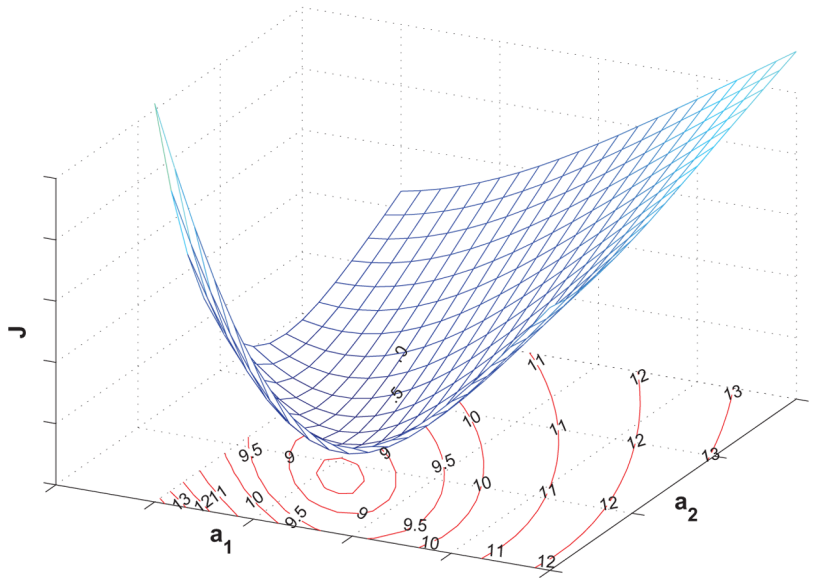

Fig. 6.
The cost function $J(a_1, a_2, h(a_1, a_2))$ vs. a_1 and a_2. It is a zoomed-in version of Figure 5.

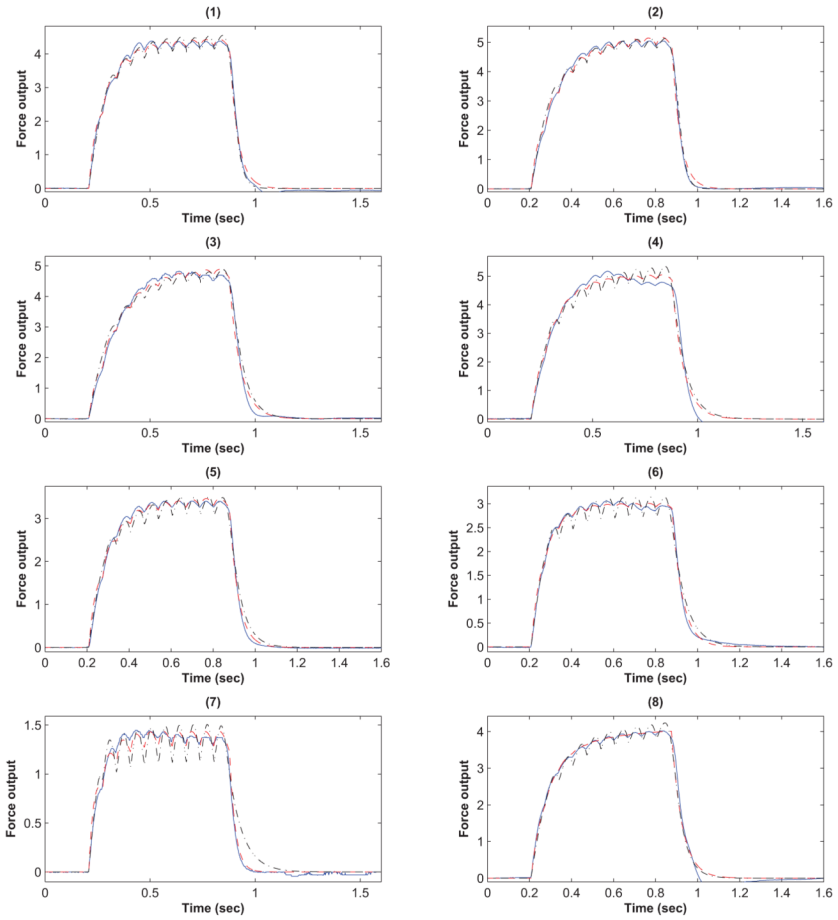

Fig. 7.

The force outputs of the Wiener-Hammerstein system (red dashed), the Hill-Huxley-type model (black dash-dotted), and the actual force output (blue solid) under 15Hz electrical stimulus for subject 1 to 8.

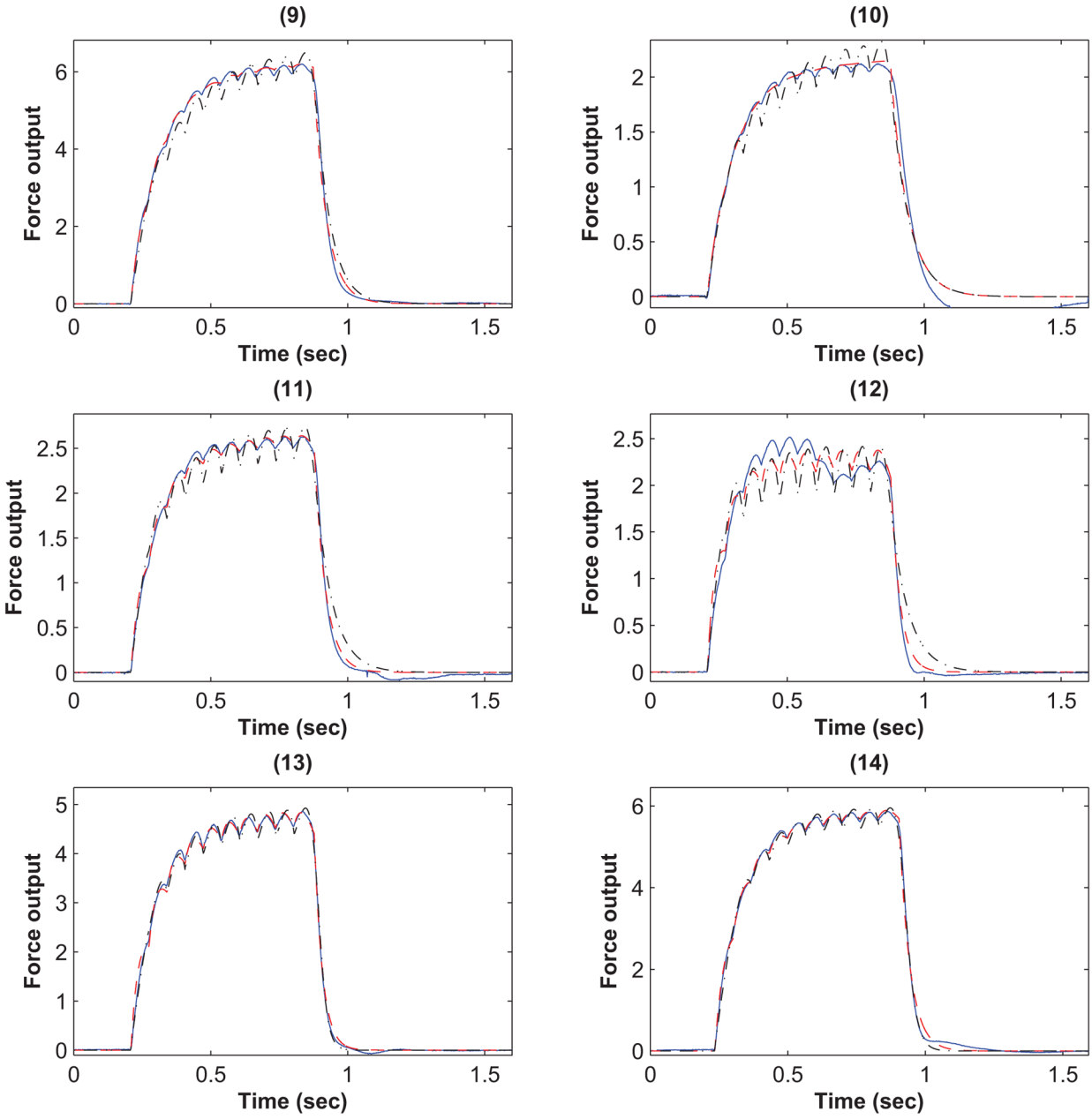

Fig. 8.

The force outputs of the Wiener-Hammerstein system (red dashed), the Hill-Huxley-type model (black dash-dotted), and the actual force output (blue solid) under 15Hz electrical stimulus for subject 9 to 14.

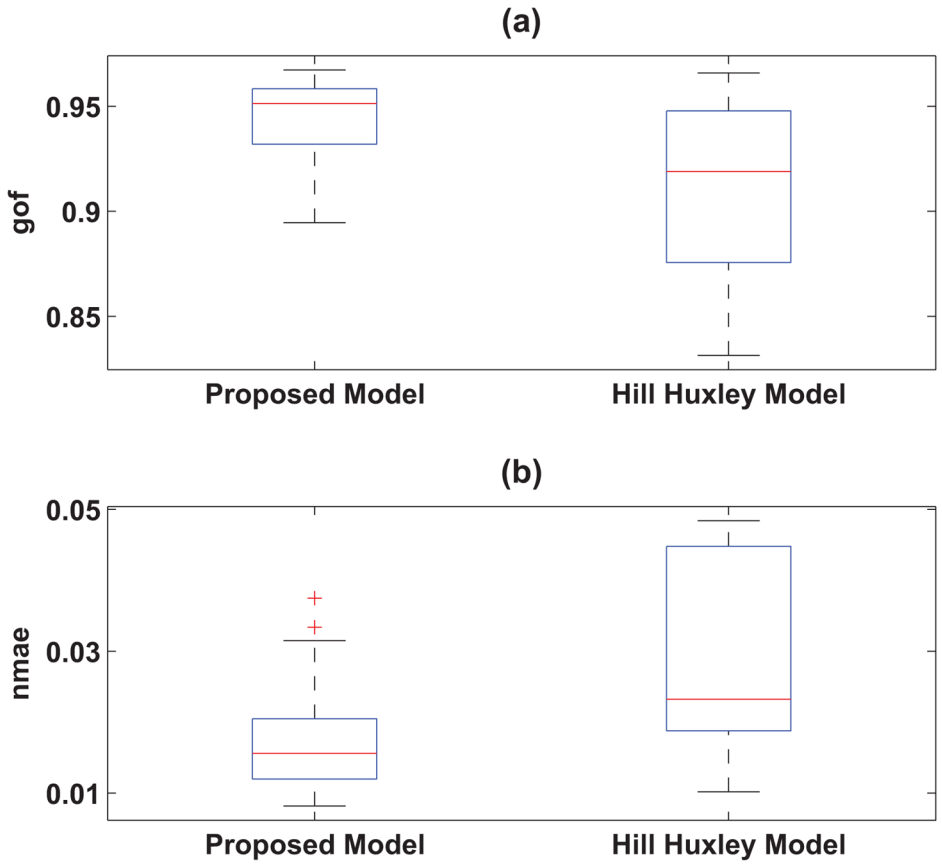

Fig. 9.
Comparison between the proposed model and Hill-Huxley-type model fitting performance in terms of (a) goodness-of-fit (gof) and (b) normalized mean absolute error (nmae).

Table 1

Goodness-of-fit (gof) and normalized mean absolute error (nmae) of the proposed modified Wiener-Hammerstein model and the Hill-Huxley-type model, respectively.

Subject	proposed model		Hill-Huxley-type model	
	gof	nmae	gof	nmae
1	0.9506	1.70%	0.9477	1.88%
2	0.9517	1.42%	0.9518	1.33%
3	0.9375	1.71%	0.9151	2.29%
4	0.8946	3.75%	0.8747	4.57%
5	0.9566	1.20%	0.9228	2.31%
6	0.9583	1.36%	0.9172	2.34%
7	0.9324	2.05%	0.8388	4.82%
8	0.9319	1.88%	0.9247	2.43%
9	0.9611	0.89%	0.9207	2.19%
10	0.8996	3.34%	0.8757	4.48%
11	0.9572	1.42%	0.9005	3.11%
12	0.8948	3.15%	0.8315	4.84%
13	0.9672	0.82%	0.9658	1.02%
14	0.9644	1.00%	0.9607	1.24%
mean	0.9388	1.84%	0.9105	2.78%

Table 2

Identified parameters of the proposed modified Wiener-Hammerstein model and the Hill-Huxley-type model.

Subject	proposed model				Hill-Huxley-type model					
	a_1	a_2	b_1	b_2	A	τ_1	τ_2	τ_c	K_m	R_0
1	0.9984	0.0090	0.9950	0.0356	45.3487	0.0243	0.1606	0.0126	0.0520	13.3251
2	0.9987	0.0041	0.9950	0.0538	45.8255	0.0209	0.1704	0.0144	0.0582	11.1040
3	0.9986	0.0042	0.9963	0.0393	38.1719	0.0537	0.1760	0.0129	0.0516	9.8250
4	0.9985	0.0096	0.9964	0.0283	45.7257	0.0593	0.1837	0.0111	0.0496	9.3385
5	0.9983	0.0075	0.9953	0.0292	35.2775	0.0506	0.1739	0.0112	0.0598	10.2671
6	0.9980	0.0495	0.9959	0.0156	36.9682	0.0629	0.1340	0.0106	0.0630	10.7141
7	0.9975	0.0104	0.9927	0.0191	24.1941	0.0663	0.2538	0.0071	0.0656	10.0867
8	0.9999	0.0360	0.9961	0.0168	37.9517	0.0439	0.2095	0.0115	0.0613	9.0618
9	0.9992	0.0183	0.9958	0.0341	49.1072	0.0530	0.2321	0.0104	0.0400	10.0303
10	1.0000	0.0436	0.9969	0.0071	18.1684	0.0650	0.2037	0.0083	0.0185	8.0968
11	0.9986	0.0140	0.9952	0.0214	26.6335	0.0608	0.2163	0.0098	0.0555	8.7164
12	0.9977	0.0151	0.9940	0.0282	31.8082	0.0637	0.2037	0.0083	0.0583	10.6444
13	0.9986	0.0085	0.9933	0.0681	44.9607	0.0180	0.2078	0.0114	0.0448	11.0869
14	0.9988	0.0158	0.9950	0.0443	54.7637	0.0234	0.1764	0.0133	0.0555	11.1727